PROBABILISTIC MODEL OF LASER RANGEFINDER

[a]MARTIN DEKAN, [b]FRANTIŠEK DUCHOŇ, [c]LADISLAV JURIŠICA, [d]ANTON VITKO

Institute of Control and Industrial Informatics
Faculty of Electrical Engineering and Information Technology
Slovak University of Technology, Ilkovičova 3
812 19 Bratislava
email: [a]martin.dekan@stuba.sk,[b]frantisek.duchon@stuba.sk,
[c]ladislav.jurisica@stuba.sk, [d]anton.vitko@stuba.sk

This work was supported by grants VMSP-P-0004-09 and KEGA 3/7307/09.

Abstract: The article deals with the design of a planar probabilistic model of laser rangefinder Hokuyo UTM-30LX which is widely used in mobile robotics. The reason for proposing such a model is the uncertainty in the distance measurements made by such sensors. Since the model is planar, the design of the model was divided into two partial models. The first partial model was established for the direction of the measurement and the second for the perpendicular direction to this measurement. The acquisition of the model parameters was carried out on the basis of numerous experiments.

Keywords: laser rangefinder, Gauss distribution, probabilistic model.

1 Introduction

Laser rangefinders are often used in many technical fields for the measuring of relative distances. They are advantageous for several reasons, such as ease of use, high accuracy, safety and efficiency. Thanks to these properties there is a wide range of potential applications of these sensors in various fields of science and industry. In the field of mobile robotics laser rangefinders are used to measure distances to obstacles around the robot. The reason for this is to provide collision-free motion and navigation in a known or unknown environment. Despite the aforementioned advantages, the measurement by a laser rangefinder is corrupted with errors. Therefore, the use of laser systems for the tasks that are performed by mobile robots (such as localization and mapping) brings for the variety of problems. These problems stem from the physical nature of the principle of laser systems operation. Consequently, their effective use requires detailed analysis of their properties and outline appropriate solutions to these problems. One solution is to improve the quality of information obtained from the laser rangefinder by the use of a mathematical model of the sensor, which this article deals with.

2 Principle of measurements using laser rangefinder

The laser rangefinder can operate on the principle of determining the time of flight (.ie. TOF) or the measurement of the phase shift between the sent and the received signal [1]. The implementation of laser rangefinders using phase shift is easier, cheaper, and therefore it is also more commonly used in practice. The laser rangefinder Hokuyo UTM-30LX, which was used in the experiments, works on the same principle. Thus, the following sections are devoted solely to this type of sensor.

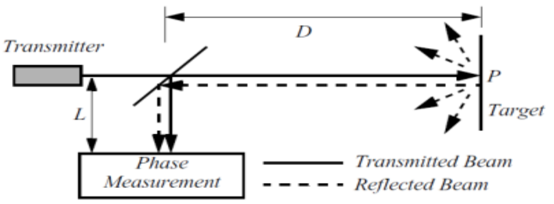

Fig. 1 Principle of laser measurement using phase shift method [1].

The measuring principle of phase shift laser rangefinder consists of sending a light beam towards the environment. The sent bordered beam of light reach the surface area of the object at point P. For a surface with a thickness greater than the wavelength of the sent light , the light reflect from the surface diffusively, which means that the reflection is nearly isotropic. The wavelength of the transmitted light in the case of the Hokuyo sensor is about 900 nm. For the majority of surfaces this means that the emitted light is reflected from them diffusively. Exceptions are only a mirror or smooth shiny surfaces such as glass. The reflected component of the light is returned back to the reader nearly in parallel when compared to the sent beam. It is obvious that the sensor emits amplitude modulated light of known frequency and measures the phase shift between the sent and the received signal. The wavelength of the modulated signal can be determined according to the equation:

$$c = f.\lambda, \tag{1}$$

where c is the speed of light and f is the modulated frequency. The total distance traveled by the light in the environment can be expressed as:

$$D' = L + 2D, \tag{2}$$

where L and D are distances defined in the picture (Fig. 1). The distance between the detector and the object can be expressed as:

$$D = \frac{\lambda}{4.\pi}\theta, \tag{3}$$

where θ is the measured phase shift between the sent and the reflected beam, λ is known wavelength of sent beam.

3 Parameters of laser rangefinder Hokuyo utm-30lx

The parameters stated by the manufacturer [2] (Table 1) are defined for a surface of exact size, situated perpendicularly to the beam of measurement. In practice it is often necessary to scan various kinds of surfaces from different angles, therefore it is necessary to experimentally verify the stated parameters for different surfaces and different angles of measurement. To complete the data necessary for the creation of the sensor model three types of experiments were performed. The first was focused on the repeatability of the measurement perpendicularly to the object, the second was aimed at the repeatability of the measurement under the angle of 45° and the third was aimed to the stability of the measurement of the edge of an object. The first two tests verify the stability of the measured distance, while the third test verifies the stability of the measured angle and the measurement on the border of two objects. The surfaces of cardboard boxes, plastic wicker surface, fabric, white paper, glossy white boards and black polished metal were used for these test.

Detection Range	Guaranteed Range: 0.1 ~ 30m (White Kent Sheet) Maximum Range : 0.1 ~ 60m
Detection Object	Minimum detectable width at 10m : 130mm (Vary with distance)
Accuracy	Under 3000lx : White Kent Sheet: ±30mm*¹ (0.1m to 10m) Under 100000lx : White Kent Sheet: ±50mm*¹ (0.1m to 10m)
Measurement Resolution	1mm

Repeated Accuracy	0.1 – 10m : σ <10mm 10 – 30m : σ <30mm (White Kent Sheet) Under 3000lx : σ = 10mm (White Kent Sheet up to 10m) Under 100000lx : σ = 30mm (White Kent Sheet up to 10m)
Scan Angle	270°
Angular Resolution	0.25° (360°/1440)
Scan Speed	25ms（Motor speed : 2400rpm）

Tab. 1 Parameters of laser rangefinder Hokuyo UTM-30LX given by the manufacturer [2].

4 Experimentally determined parameters of sensor model

Based on data gathered from the measurement (Fig. 2) , the Gaussian sensor model was chosen as the most suitable probabilistic model for our sensor[3].

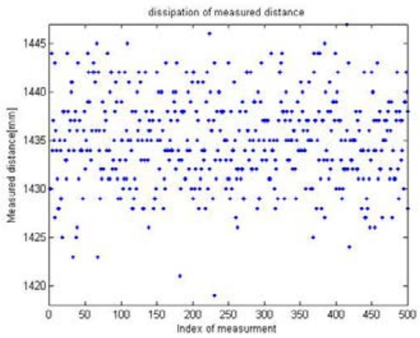

Fig. 2 Example of data set measurement which where used in the probabilistic model.

The probability distribution of measured distances in the Gaussian model equal to:

$$f(x) = \frac{1}{\sqrt{2\pi\sigma^2}} e^{-\frac{(x-\mu)^2}{2\sigma^2}}, \tag{4}$$

where σ is the standard deviation and μ is the average distance of measurements.

For each surface, listed in the previous section, 20 experiments of 500 measurements of a selected distance were carried out. Measurements were conducted perpendicularly to the surface or at an angle of 45 °.

1. *Cardboard box* - was characterized by the most stable measurement. In perpendicular measurements (Fig. 3 left) the standard deviation was $\sigma = 4{,}6533$ mm. The measurements at an angle of 45 ° (Fig. 3 right) showed significantly lower quality with a standard deviation of $\sigma = 5{,}9321$ mm.

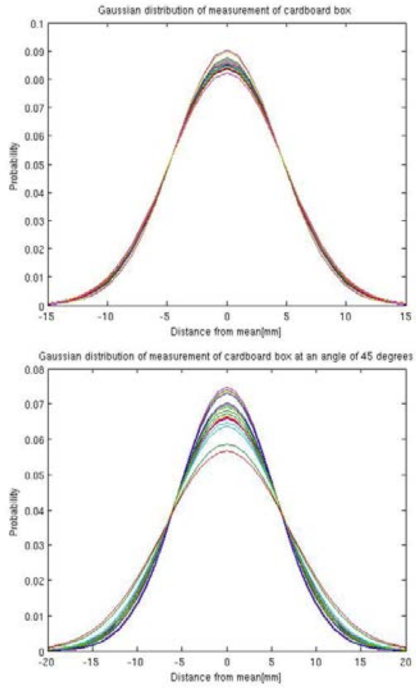

Fig. 3 The Gaussian distribution of distance measurementof cardboard box perpendicular to the surface (left) at an angle of 45° (right) .

2. *Plastic wicker surface* - Plastic wicker surface - for the distance measured perpendicular to that surface (Fig. 4 left) characteristics of measurements were similar to those of the cardboard box. The standard deviation was equal to $\sigma = 4{,}9129$ mm. As for the measuring this surface at an angle of 45 ° (Fig. 4 right) the heterogeneous structure of the surface was shown significantly. Thus the repeatability of the measurement was worsened as well. The standard deviation for this measurement was equal to $\sigma = 5{,}6927$.

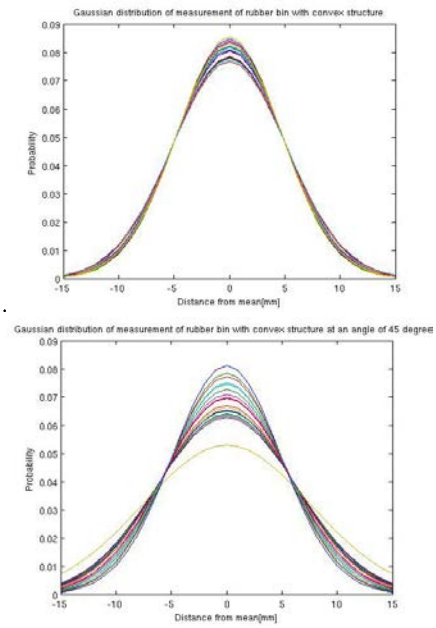

Fig. 4 The Gaussian distribution of distance measurement of plastic wicker surface perpendicular to the surface (left) at an angle of 45° (right).

3. *Fabric* - for the measurement of the fabric surface in the perpendicular direction (Fig. 5 left) the standard deviation was $\sigma = 4{,}9352$ mm. This surface shows a small variance of values. By the measurements at an angle of 45 ° (Fig. 5 right) large fluctuations between individual measurements emerged in the data set. The standard deviation of this measurement was $\sigma = 6{,}1049$.

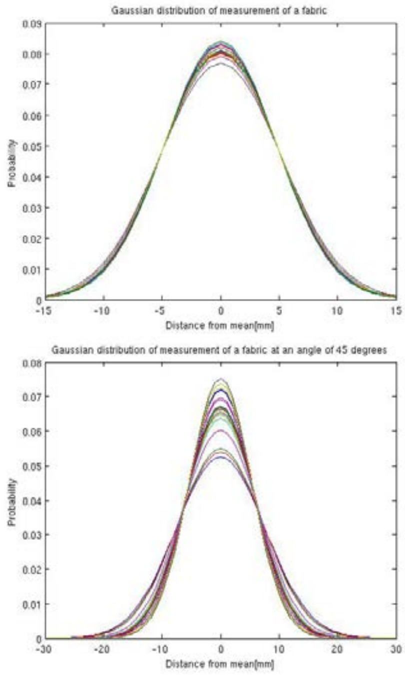

Fig. 5 The Gaussian distribution of distance measurementof fabric perpendicular to the surface (left) at an angle of 45° (right).

4. *White paper* - for the measurements of this surface in the perpendicular direction (Fig. 6 left) the standard deviation of $\sigma = 5{,}3914$ mm has the highest value of all surfaces. Similarly, for the measurements at an angle of 45° (Fig. 6 right) white paper is the surface showing the worst measurement repeatability. The value of the standard deviation for these measurements was $\sigma = 6{,}2753$ mm.

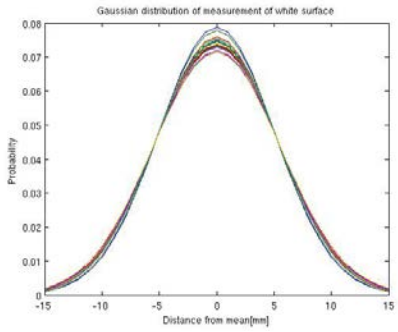

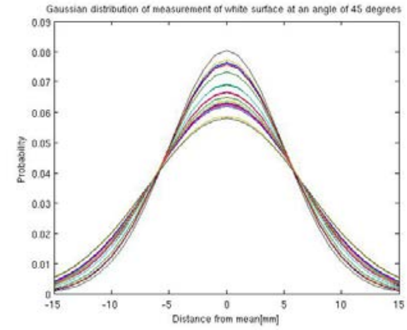

Fig. 6 The Gaussian distribution of distance measurementof white paper perpendicular to the surface (left) at an angle of 45° (right).

5. *White shiny surface* - White shiny surface - this type of surface belonged to the surfaces with the worst measurement repeatability for the measurements in the perpendicular direction (Fig. 7 left) , similarly to the white paper,. The standard deviation for these measurements was $\sigma = 5{,}0832$ mm. The standard deviation for the measurements at an angle of 45 ° (Fig. 7 right) was $\sigma = 5{,}8775$ mm.

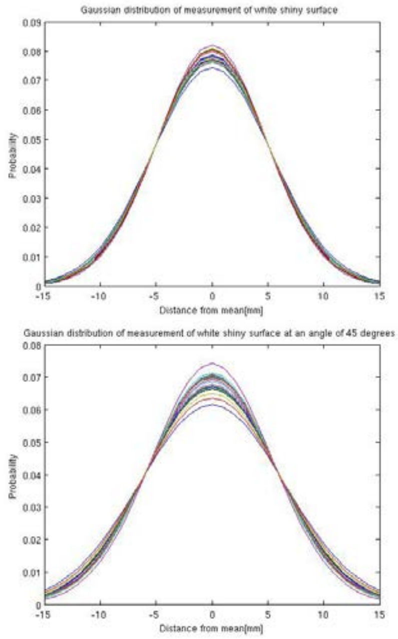

Fig. 7 The Gaussian distribution of distance measurementof white shiny surface perpendicular to the surface (left) at an angle of 45° (right).

6. *Shiny black metal* - Shiny black metal - the perpendicular measurements of the black shiny metal surface (Fig. 8 left) were the measurements with one of the highest repeatability. Standard deviation was $\sigma = 4{,}7402$ mm. For the measurements at an angle of 45° (Fig. 8 right), the surface showed a mirror reflection of signals transmitted by the sensor, and therefore the standard deviation had a value of $\sigma = 8{,}6743$ mm.

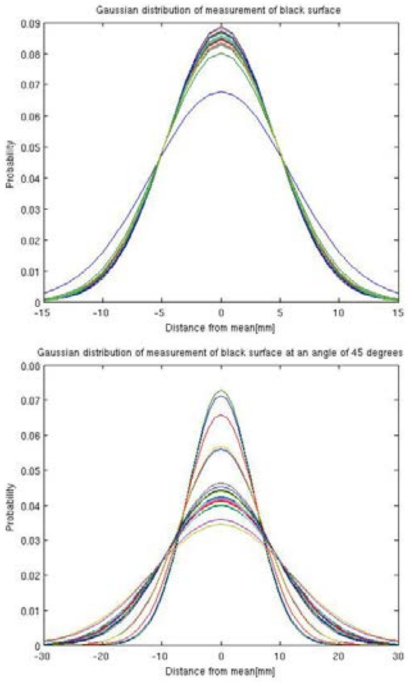

Fig. 8 The Gaussian distribution of distance measurementof shiny black metal surface perpendicular to the surface (left) at an angle of 45° (right).

Type of the surface	**Perpendicular measurement**	**Measurement at an angle of 45°**
Cardboard box	**4,6533 mm**	5,9321 mm
Plastic wicker surface	4,9129 mm	**5,6927 mm**
Fabric	4,9352 mm	6,1049 mm
White paper	**5,3914 mm**	6,2753 mm
White shiny surface	5,0832 mm	5,8775 mm
Shiny black metal	4,7402 mm	**8,6743 mm**

Tab. 2 Comparison of all standard deviations for all measurements. The highest values of the various types of measurements are highlighted in red, the lowest in blue.

In the third type of experiments the cardboard box was used because of the best results for perpendicular measurements. The measurement was aimed at the consistency of data around the edges of obstacles, i.e. the determination of the position of an obstacle within the measured data set (Fig. 9). The measurement was taken for four distances - 50 cm, 150 cm, 250 cm and 530 cm. For each distance, measurements were performed 10 times with 500 measured distances per data set. The measurement result is the number of shifts of the object for its left and right edge. The results are shown in the table (Table 3).

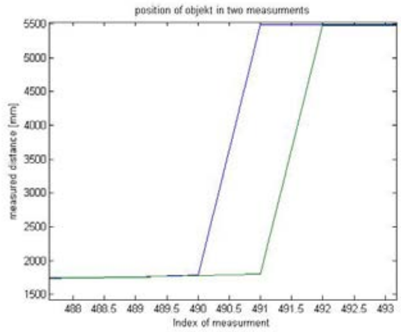

Fig. 9 Example of the position of the object boundary shift between the two measurements.

Measured distance / Number of measureme	1	2	3	4	5	6	7	8	9	10
50 cm	161	246	197	220	180	190	146	108	136	248
150 cm	191	27	105	211	85	90	60	31	180	33
250 cm	44	43	48	38	160	74	39	5	142	18
530 cm	5	32	34	0	42	74	14	2	1	0

Tab. 3 Number of the boundary shifts of the object at the corresponding measured distances from the total number of 500 measurements.

The Gaussian distribution was determined for the given measurement set (Fig. 10). As can be seen, with increasing distance the shift of boundaries of an object tends to decrease. This is due to the wider dispersion of the transmitted rays.

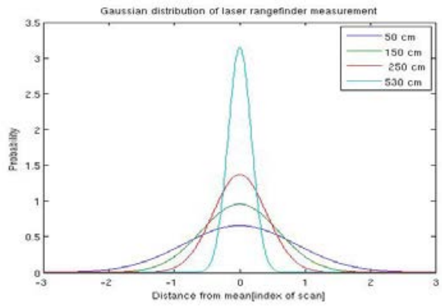

Fig. 10 Gaussian distribution of distance measurements to a cardboard box for object boundaries shift.

Based on the Gaussian distribution and the measured distances it is possible to determine the shift of the object border on the basis of angular distances between two beams of the laser range finder (Table 4) according to:

$$y = 3.\sigma.\sin(d).dst\,, \qquad (5)$$

Measured distance	**σ [mm]**	**y [mm]**
50 cm	0,6078	3,9783
150 cm	0,4160	8,1677
250 cm	0,2907	9,5131
530 cm	0,1269	8,8020

Tab. 4 Standard deviation of Gaussian distributions for various measured distances and their corresponding distances for the boundaries shift of the object.

5 Sensor Model

The complete sensor model is composed of two partial models derived in Chapter 4. The laser rangefinder Hokuyo UTM-30LX is a planar rangefinder (i.e. measures distances in the plane), and therefore it must be interpreted, as well as its measurement, in the plane. As the partial model in the direction of the measured distance, we used the model derived by measuring the distances to objects (first and second test or type of measurement). In this case, the Gaussian distribution with the average of standard deviations of all types of measurements was chosen. Its value is equal to $\sigma = 5{,}6894$ mm. The resulting Gaussian distribution is shown in Fig. 11.

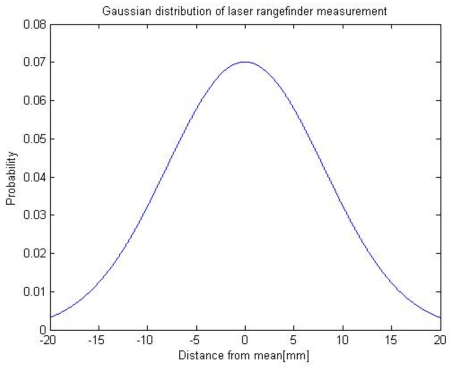

Fig. 11 The final Gaussian distribution model for the Hokuyo UTM LX-30 sensor in the direction of a measured distance.

As the model in the direction perpendicular to the direction of distance measurements, the model derived from the shift of object boundaries was chosen. The resulting standard deviation for the Gaussian distribution in this direction was $\sigma = 3$ mm. The resulting distribution can be seen in Fig. 12.

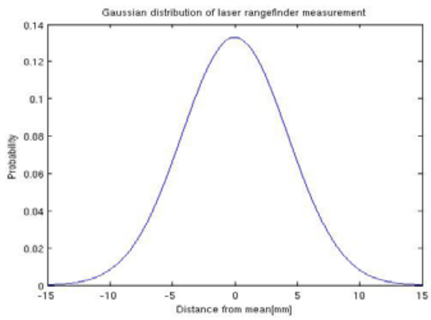

Fig. 12 The final Gaussian distribution model for the Hokuyo UTM LX-30 sensor in a direction perpendicular to the measured distance.

Based on these two resultant Gaussian distribution the resulting model of laser range finder has been created (Fig. 12):

$$f(x,y) = \frac{1}{2\pi\sqrt{\sigma_x^2\sigma_y^2}} e^{-\left(\frac{(x-\mu_x)^2}{2\sigma_x^2}+\frac{(y-\mu_y)^2}{2\sigma_y^2}\right)}, \qquad (6)$$

where x is the corresponding measured distance, the σ_x is standard deviation of the Gaussian distribution in the direction of the measured distance, y is the corresponding dispersion distance in a direction perpendicular to the measured distance (see Table 4. and the formula 5) and σ_y is the standard deviation of the Gaussian distribution in the direction perpendicular to the measured distance.

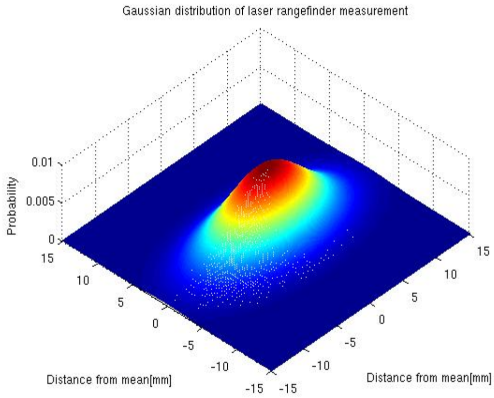

Fig. 13 The resulting planar Gaussian model of the laser rangefinder Hokuyo UTM-30LX sensor.

For the purposes of mobile robotics, such as area mapping, the model of laser rangefinder can be specified in tabular form, or grid. For a selected raster of 5x5 mm (i.e. the size of a cell in metric maps is 5 mm) and for the derived sensor model, such a table is:

0,0124	0,1629	0,0124
0,0414	0,5416	0,0414
0,0124	0,1629	0,0124

Tab. 5 Example of a tabular representation of the sensor model.

The application of the sensor model can be explained on a simple example. Let the measured distance be 200 mm. Let us say that the beam, that measured this distance, was sent at an angle of 0 °. Then in the environment map, for the position x = 40, y = 0, the probability that the cell is occupied will have a value equal to 0,5416, the neighboring cell at the position x = 41, y = 0 will have the value of probability of occupation 0,1629 etc.

6 Conclusion

The proposed probabilistic model can be used on various areas of practice. At the workplace URPI FEI STU it is used primarily for mobile robot control. Mobile robots perform foremost tasks of localization and navigation. Since most of the available sensors are inaccurate, it is necessary to use information fusion from different sensors. For this it is necessary to have a good sensor model. The proposed model can be used in localization (e.g. Markov or using the Kalman filter) as well as for navigation (e.g. the creation of a probabilistic representation of the grid environment) of a mobile robot.

Literature:

1. Siegwart, R., Nourbakhsh, I.R. *Introduction to Autonomous Mobile Robots*. Massachusetts Institute of Technology, 2004. 336p. ISBN-13 978-0-262-19502-7.
2. *Scanning Laser Range Finder UTM-30LX/LN Specification*. Available at: http://www.hokuyo-aut.jp/02sensor/07scanner/download/data/UTM-30LX_spec.pdf
3. Greš, J., Kelemen, M.: *Model of biologically inspired robot Spinner*. Strojárstvo 1/2007, p. 72-73. ISSN 1335-2938.

Primary Paper Section: J

Secondary Paper Section: JB,JD